ACS APPLIED MATERIALS & INTERFACES

Research Article

www.acsami.org

Physical Tuning of Cellulose-Polymer Interactions Utilizing Cationic Block Copolymers Based on PCL and Quaternized PDMAEMA

Simon Utsel,*[,†,§] Carl Bruce,[†,§] Torbjörn Pettersson,[†] Linda Fogelström,[†] Anna Carlmark,[†] Eva Malmström,[†] and Lars Wågberg[†,‡]

[†]Department of Fibre and Polymer Technology, KTH Royal Institute of Technology, Teknikringen 56, SE-100 44 Stockholm, Sweden

[‡]Wallenberg Wood Science Centre, KTH Royal Institute of Technology, Teknikringen 56, SE-100 44 Stockholm, Sweden

Supporting Information

ABSTRACT: In this work, the objective was to synthesize and evaluate the properties of a compatibilizer based on poly(ε-caprolactone) aimed at tuning the surface properties of cellulose fibers used in fiber-reinforced biocomposites. The compatibilizer is an amphiphilic block copolymer consisting of two different blocks which have different functions. One block is cationic, quaternized poly(2-(dimethylamino)ethyl methacrylate) (PDMAEMA) and can therefore electrostatically attach to anionic reinforcing materials such as cellulose-based fibers/fibrils under mild conditions in water. The other block consists of poly(ε-caprolactone) (PCL) which can decrease the surface energy of a cellulose surface and also has the ability to form physical entanglements with a PCL surface thereby improving the interfacial adhesion. Atom Transfer Radical Polymerization (ATRP) and Ring-Opening Polymerization (ROP) were used to synthesize three block copolymers with the same length of the cationic PDMAEMA block but with different lengths of the PCL blocks. The block copolymers form cationic micelles in water which can adsorb to anionic surfaces such as silicon oxide and cellulose-model surfaces. After heat treatment, the contact angles of water on the treated surfaces increased significantly, and contact angles close to those of pure PCL were obtained for the block copolymers with longer PCL blocks. AFM force measurements showed a clear entangling behavior between the block copolymers and a PCL surface at about 60 °C, which is important for the formation of an adhesive interface in the final biocomposites. This demonstrates that this type of amphiphilic block copolymer can be used to improve interactions in biocomposites between anionic reinforcing materials such as cellulose-based fibers/fibrils and less polar matrices such as PCL.

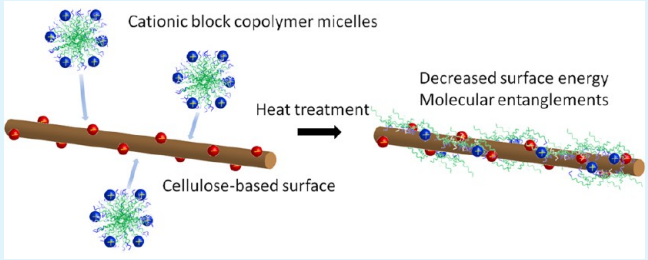

KEYWORDS: *compatibilizer, biocomposite, cellulose, poly(ε-caprolactone), cationic micelle, block copolymer*

INTRODUCTION

One of the main functions of cellulose in nature is as a load-bearing component in plants and trees. The idea of using cellulose-based materials as a reinforcing component in biocomposites is therefore not unreasonable, and it can be considered as a biomimetic material. Cellulose-based materials, such as micrometer-sized fibers and nanometer-sized fibrils/whiskers, are interesting for biocomposite applications due to their good mechanical properties, high aspect ratio, relatively low density, biorenewability, and biodegradability.[1] However, due to the relatively hydrophilic nature of cellulose the compatibility with many polymer matrices is poor, and this leads to insufficient mechanical properties of the final materials.[2−4] Significant efforts both in industry and in academia have therefore aimed at improving this compatibility, usually by modifying the cellulose surface.[5−8] Two of the main challenges are to obtain a homogeneous dispersion of the reinforcing material in the polymer matrix and to improve the stress-transfer between the reinforcing material and the polymer matrix. The dispersion can be significantly improved by decreasing the surface energy of the reinforcing material so that it better matches the surface energy of the polymer matrix. The stress-transfer can be improved by improving the adhesion at the interface between the reinforcing material and the polymer matrix.[9] One chemical approach that has shown to improve the mechanical properties of a cellulose-based biocomposite is to covalently graft the same kind of polymer that is used as the polymer matrix from the cellulose surface.[10] This can both decrease the surface energy of the cellulose-based reinforcing material as well as improve the adhesion to the matrix by introducing chain entanglements across the interface. The molecular weight of the entangling block at the interface has in earlier work been shown to have a great influence on the adhesion between the two different phases,[10,11] and it is therefore an important parameter to consider.

Received: September 13, 2012
Accepted: November 16, 2012
Published: November 16, 2012

The development of controlled polymerization techniques has significantly increased the availability of tailor-made polymers with controlled molecular weight, low dispersity, and known chain-end functionalities. For instance, Atom Transfer Radical Polymerization (ATRP),[12] has proven to be a widely used, versatile method especially since a broad range of monomers can be polymerized and all mediating agents are commercially available. Even more interestingly, the use of ATRP also facilitates the synthesis of well-defined block copolymers.[13−15]

Well-defined polymers is of outmost importance for a range of applications, such as surfactants for colloidal systems,[16] micelles used for delivery of bioactive compounds,[17] and as compatibilizers of immiscible blends, such as between a hydrophobic matrix and a hydrophilic reinforcing material.[18,19] In the latter study it was shown that a block copolymer based on polystyrene and a cationically charged block of poly(2-(dimethylamino)ethyl methacrylate) (PDMAEMA) decreased the surface energy of a cellulose surface as well as substantially improved the adhesion toward a polystyrene surface.

In another study by Lönnberg et al.[20] it was demonstrated that the interfacial toughness between a film of microfibrillated cellulose and poly(ε-caprolactone) (PCL) could be tailored by grafting PCL of various lengths from the surface of microfibrillated cellulose by Ring-Opening Polymerization (ROP).[21] It was shown that the interfacial peeling toughness correlated strongly with the length of the PCL-grafts, due to physical entanglements. However, this approach suffers from the experimentally challenging surface modification where PCL is grafted *from* the surface of cellulose.

Inspired by these previous studies we designed a novel block copolymer with the purpose to circumvent the tedious grafting *from* step while maintaining the tailorable interfacial toughness. A series of block copolymers composed of one cationically charged block of quaternized PDMAEMA, obtained by ATRP, and one block of PCL, made with ROP was synthesized, adopting the synthetic procedures from Jakubowski et al.[22] and Motala-Timol and Jhurry.[23] In a final step, the PDMAEMA-block was quaternized, resulting in a cationically charged block to promote the adsorption to an oppositely charged surface, such as a cellulose-based fiber/fibril surface.[18] As discussed above, the PCL-block reduces the surface energy of the surface to which it is adsorbed, so that it becomes more compatible with a PCL surface, and also improves the adhesion to a PCL surface by allowing polymer entanglements to form across the interface. This approach can be considered as a physical alternative to covalent surface modification.[10,24] The main advantage of this approach is that the polymers can be synthesized separately and then adsorb to fibers/fibrils in water under mild conditions. PCL was used since it is a biodegradable material that has gained increasing interest during recent years.[25] Earlier work has shown that an improved compatibility between PCL and cellulose-based materials leads to improved mechanical properties of the final biocomposites.[10]

To the best of the authors knowledge, the PDMAEMAq-*block*-PCL has only sparsely been described in the literature,[22,23] never before been utilized as a compatibilizer and subjected to a systematic evaluation. This type of surface modification could expand the use of cellulose-based reinforcing materials for biocomposite applications.

EXPERIMENTAL SECTION

Materials. 2-(Dimethylamino)ethyl methacrylate (DMAEMA, 98%, Aldrich) was passed through a basic Al_2O_3 column prior to use to remove the inhibitor. ε-Caprolactone (ε-CL, 99%, Alfa Aesar) was dried over CaH_2, distilled under reduced pressure, and stored under argon. Toluene (HPLC grade, Fischer Scientific) was dried prior to use. Hydroxyethyl bromoisobutyrate (HEBI, 95%, Aldrich), 1,1,4,7,10,10-hexamethyltriethylenetetramine (HMTETA, 97%, Aldrich), copper chloride (Cu(I)Cl, (99+ %, Aldrich), tin octoate ($Sn(Oct)_2$, 95%, Aldrich), acetone (Prolabo, technical), methanol (MeOH, Merck), ethanol (EtOH, 95%, VWR), tetrahydrofuran (THF, Merck), dichloromethane (DCM, Merck), dimethyl sulfoxide (DMSO, 99.9%, Sigma), *N*-methylmorpholine N-oxide (NMMO, 97%, Sigma), aminopropyl triethoxysilane (APTES, 98%, Aldrich), hydrochloric acid (HCl, 37%, Acros organics), and methyl iodide (MeI, 99%, Lancaster) were all used as received. Borosilicate glass microspheres 10 μm in diameter (Thermo Scientific, CA) were used for AFM force measurements. Polyethyleneimine (PEI) (Acros Organics, 50 wt % aqueous solution) with a molecular weight of 60 kDa was used for the preparation of cellulose model surfaces. Nanofibrillated cellulose (NFC) was prepared at Innventia AB, Stockholm, Sweden. The procedure was similar to an earlier described high-pressure homogenizer technique[26,27] but with a different high-pressure homogenizer and a new pretreatment of the wood fibers.[28] The pulp used for NFC preparation was produced from a commercial sulfite softwood dissolving pulp (Domsjö Dissolving Plus; Domsjö Fabriker AB, Domsjö, Sweden) based on 60% Norwegian spruce (*Picea abies*) and 40% Scots pine (*Pinus sylvestris*), and the fibrils were used in their never-dried form. Ultra pure water (Milli-Q) was used for all measurements.

Methods. Proton nuclear magnetic resonance (^{1}H NMR) spectra was recorded with a Bruker AM 400 using deuterated chloroform ($CDCl_3$) as solvent. The residual solvent signal was used as the internal standard.

Molecular weight (M_n) and dispersity ($Đ_M$) were determined with Size Exclusion Chromatography (SEC) with a TOSOH EcoSEC HLC-8320GPC system equipped with an EcoSES RI detector and three columns (PSS PFG 5 μm; Microguard, 100 Å and 300 Å) (MW resolving range: 300−100 000 Da) from PSS GmbH, using DMF (0.2 mL min^{-1}) with 0.01 M LiBr as the mobile phase at 50 °C. A conventional calibration method was created using narrow linear poly(methyl methacrylate) standards. Corrections for flow rate fluctuations were made using toluene as an internal standard. PSS WinGPC software version 7.2 was used to process the data.

The thermal properties of the polymers were analyzed with a Differential Scanning Calorimeter (DSC). The experiments were performed with a Mettler-Toledo DSC with Mettler Toledo STARe software V9.2 equipped with a sample robot and a cryo-cooler. The heating and cooling rates were 10 °C min^{-1} in the temperature range of −60 to 160 °C. PCL is a semicrystalline polymer, and it is therefore possible to study the crystallization behavior of the block copolymers. The degree of crystallinity (X_c) was calculated according to

$$X_c = \frac{\Delta H_c}{\Delta H^\circ_{100}} \quad (1)$$

where ΔH_c is the heat of crystallization of the sample, and ΔH°_{100} is the heat of crystallization of 100% crystalline PCL, which has a value of 136.4 J/g.[29]

Dynamic Light Scattering (DLS) (Malvern Zetasizer NanoZS) was used to determine the hydrodynamic radius of the block copolymer micelles in water. 100 mg/L dispersions were prepared without addition of salt, having a pH about 8.

Cryo-TEM was performed with a Philips CM120 cryo-TEM operated at 120 kV and equipped with a cryo holder (Oxford Instruments CT-3500). Images were recorded with a GIF 100 (Gatan imaging filter). Samples were prepared in a CEVS (controlled environment vitrification system) and freeze plunged into liquid ethane (−180 °C) and then stored in liquid nitrogen. Lacey carbon

filmed Cu grids were used as substrate, and the concentration of the dispersions was 1 g/L.

Polyelectrolyte Titration (PET) was used to measure the charge density of the block copolymer micelles using a 716 DMS Titrino (Metrohm, Switzerland) with potassium poly(vinyl sulfate) (KPVS) as the titrant and orthotoluidine blue (OTB) as the indicator. The color change was recorded spectroscopically with a Fotoelektrischer Messkopf 2000 (BASF), and the amount of KPVS needed to reach equilibrium was calculated according to Horn et al.[30]

Silicon oxide surfaces and cellulose model surfaces were both used as substrates for the adsorption of the cationic block copolymers. Silicon wafers (p-type, MEMC Electronics Materials, Novara, Italy), with naturally occurring silicon oxide surfaces, were rinsed with Milli-Q water, ethanol, and Milli-Q water and blown dry with N_2. The wafers were then placed in an air plasma cleaner (Model PDC 002, Harrick Scientific Corporation, NY, USA) under reduced air pressure at high effect (30 W) for 120 s, after which the wafers were ready for use.

Cellulose model surfaces were prepared as follows. A silicon wafer treated as described above was used to assemble the cellulose model surface using the Layer-by-Layer (LbL) technique. Two bilayers were assembled using 100 mg/L solution/dispersion of PEI/NFC using a method similar to that described earlier.[31]

A Quartz Crystal Microbalance with Dissipation Monitoring (QCM) E4 from Q-Sense AB (Västra Frölunda, Sweden) was used to study the block copolymer adsorption to the solid−liquid interface with a continuous flow of 100 μL/min.[32] The substrates were AT-cut quartz crystals with an active surface of sputtered silicon oxide cleaned in the same way as the silicon wafers described above. 100 mg/L dispersions without added salt with a pH about 8 were used for all adsorption steps in this work. The change in frequency depends on the adsorbed mass according to the Sauerbrey model[33]

$$m = C\frac{\Delta f}{n} \tag{2}$$

where m = adsorbed mass per unit area [mg/m^2], C = sensitivity constant, −0.177 [mg/m^2·Hz], Δf = change in resonant frequency [Hz], and n = overtone number.

This model assumes rigidly attached layers, and the adsorbed amount contains both polymer and water coupled to the adsorbed layer. However, earlier work has shown that this model is comparable to more advanced models also for layers with higher dissipation.[34]

An Atomic Force Microscope (AFM) MultiMode IIIa (Veeco Instruments Inc. Santa Barbara, CA) was used for imaging and adhesion measurements. For tapping mode imaging in air, an EV scanner was employed using standard noncontact mode silicon cantilevers with a spring constant in the range of 32 to 70 N/m (TAP150, Bruker, Camarillo, CA). The colloidal probe[35,36] adhesion measurements were performed by capturing normal force curves in air using a high temperature heater accessory (HJV scanner). For the force curves tipless rectangular cantilevers (NSC12, MicroMasch, Madrid, Spain) approximately 110 μm in length and 35 μm in width, and with normal spring constants in the range of 3.5−12.5 N/m, were used. The exact values of the normal spring constants were determined by a method based on thermal noise with hydrodynamic damping[37] using the AFM tune IT v 2.5 software (Force IT, Sweden). The thermal frequency spectra of the cantilevers were measured at room temperature without any particles attached.[38] A silica particle (Thermo scientific, CA) with a diameter of approximately 10 μm was attached with a manual micromanipulator and an Olympus reflection microscope to the end of the tipless cantilever, using a small amount of a two-component epoxy adhesive (Strong epoxy rapid, Casco). The silica particles were modified with the different block copolymers by first plasma treating the silica particles after attachment to the cantilever, adsorbing the block copolymers in 100 mg/L polymer solutions and finally heat-treating them at 160 °C.

Contact angles were measured at 50% RH and 23 °C on a KSV instrument CAM 200 equipped with a Basler A602f camera, using 5 μL droplets of Milli-Q water.

Synthesis of PDMAEMA-OH (PDMAEMA Macroinitiator). Destabilized DMAEMA (20.0 g, 127 mmol) was added to a 50 mL round-bottomed flask, equipped with a stir bar, and dissolved in acetone (20.0 g). HEBI (360 mg, 1.7 mmol) and HMTETA (780 mg, 3.4 mmol) were subsequently added, and the flask was closed with a rubber septum. The flask was evacuated and backfilled with argon gas. Thereafter, the septum was carefully removed and Cu(I)Cl (170 mg, 1.7 mmol) was added, after which the septum was reattached and two more vacuum/argon cycles were performed. The flask was immersed in an oil bath preheated to 50 °C, and the reaction was allowed to proceed for 1 h whereafter the reaction mixture was allowed to cool to ambient temperature under exposure to air, and THF was added to dissolve the polymer formed. The polymer solution was passed through an activated, neutral Al_2O_3 column to remove the copper and was thereafter precipitated in a 10-fold excess of cold heptane (−78 °C). The polymer, PDMAEMA-OH, was recovered via filtration and dried under reduced pressure at room temperature for 24 h, followed by ^{1}H NMR, SEC, and DSC analysis.

Synthesis of PDMAEMA-*block*-PCL (from PDMAEMA-OH, Macroinitiator). Three target degrees of polymerization (DP) of PCL were aimed for: 300, 1200, and 2400 which were denoted PDMAEMA-*block*-PCL-s (short), PDMAEMA-*block*-PCL-m (medium), and PDMAEMA-*block*-PCL-l (long), respectively.

All three polymerizations of PCL from the PDMAEMA-OH (macroinitiator) were carried out according to the general procedure described hereafter. A 50 mL round-bottomed flask equipped with a stir bar was dried in an oven at 150 °C overnight and flame-dried prior to use. Toluene (50 g) was added together with ε-CL, as indicated in Table 1, where half the toluene was distilled off to remove residual traces of water. The flask was equipped with a rubber septum, and three cycles of evacuation and backfilling with argon gas followed. A separate glass vial was flame-dried and cooled, followed by the addition of PDMAEMA-OH as in Table 1. The vial was thereafter equipped with a stir bar and a septum and flushed with argon gas for 10 min. Toluene (5 g) and $Sn(Oct)_2$ (0.45 eq. compared to the total amount of PDMAEMA-OH added) was added, and the macroinitiator was dissolved under stirring and flushing with argon at room temperature for 30 min. The macroinitiator solution was then transferred into the 50 mL round-bottomed flask, which was subsequently immersed into a preheated oil bath set to 85 °C. The reaction was conducted for times indicated in Table 1. Thereafter, the reaction mixture was cooled to room temperature, diluted with THF, and precipitated in a 10-fold excess of cold MeOH (−78 °C). The block copolymer was then filtered off, dried under reduced pressure at room temperature overnight, and finally analyzed with ^{1}H NMR, SEC, FT-IR, and DSC.

Table 1. Added Amounts of Reactants and Reaction Times for the Polymerizations

sample	DP target	PDMAEMA	ε-CL	reaction time
PDMAEMA-*block*-PCL-s	300	250 mg, 71.4 μmol	2.40 g, 21.4 mmol	75 h
PDMAEMA-*block*-PCL-m	1200	250 mg, 71.4 μmol	9.80 g, 85.7 mmol	91 h
PDMAEMA-*block*-PCL-l	2400	250 mg, 71.4 μmol	19.6 g, 172 mmol	113 h

Quaternization of PDMAEMA-*block*-PCL. The quaternization of the PDMAEMA-*block*-PCL block copolymer was conducted in the same manner for all three block copolymers. A 50 mL round-bottomed flask was equipped with a stir bar followed by the addition, as indicated in Table 2, of block copolymer and THF to dissolve the block copolymer. MeI was added to a vial and dissolved in THF in amounts as in Table 2. The MeI solution was then subsequently added dropwise to the flask containing the block copolymer solution. The reaction was left to proceed overnight at room temperature. A gel-like consistency was noted. DCM was added to dissolve the block copolymer, which was thereafter precipitated in a 10-fold excess of cold heptane (−78 °C). The quaternized block copolymer was

Table 2. Added Amounts for Quaternization of the Block Copolymers

sample	PDMAEMA-*block*-PCL	THF[b]	MeI	THF[c]
PDMAEMA-*block*-PCL-s	3.0 g, 6.1 mmol[a]	12 g	162 mg, 1.15 mmol	6 g
PDMAEMA-*block*-PCL-m	4.0 g, 5.6 mmol[a]	16 g	216 mg, 1.50 mmol	8 g
PDMAEMA-*block*-PCL-l	8.0 g, 5.5 mmol[a]	32 g	216 mg, 1.50 mmol	16 g

[a]The amount of PDMAEMA in PDMAEMA-*block*-PCL calculated from molecular weights from SEC. [b]Amount of THF used to dissolve the PDMAEMA-block-PCL. [c]Amount of THF mixed with MeI prior to adding it to the block copolymer.

recovered via filtration, dried under reduced pressure at room temperature overnight, and analyzed with PET. After quaternization, the block copolymers were denoted PDMAEMAq-*block*-PCL-s, PDMAEMAq-*block*-PCL-m, and PDMAEMAq-*block*-PCL-l.

Micelle Formation. The three PDMAEMAq-*block*-PCL polymers were transformed into micelles according to the following procedure. Each polymer (100 mg) was separately dissolved in DMF (10 g), and the solutions were added dropwise under stirring to a flask with Milli-Q water (90 g). The mixtures were then dialyzed against Milli-Q water for three days, using dialysis tubing with a 6000−8000 Da cutoff (Spectrum Laboratories Inc., CA), and the water was continuously replaced with fresh Milli-Q water.

RESULTS AND DISCUSSION

In this study, PCL-based cationic block copolymers were synthesized, with varying lengths of the PCL block. Their properties in solution and at the solid−liquid interface were investigated as well as their adhesive properties to a PCL surface.

PCL was chosen since it is an interesting biodegradable material and because polymerization methods, e.g. ROP, are available to synthesize well-defined PCL-based structures, which is essential in this kind of study aiming at a molecular understanding of adhesive phenomena. There is also significant room for improvement of PCL-based composites by tuning the interfaces in the final biocomposites.[10] PDMAEMA was chosen as the base for the charged block since it is readily synthesized *via* ATRP in a controlled manner,[39] and the resulting polymer can be quaternized using MeI, resulting in a cationically charged polyelectrolyte. Furthermore, quaternized PDMAEMA has previously been demonstrated to readily adsorb onto cellulose substrates.[18]

POLYMER PREPARATION

Three well-defined PDMAEMA-*block*-PCL copolymers were synthesized through combining the two controlled polymerization techniques, ATRP and ROP. The block copolymers were prepared in a three-step process; first, a PDMAEMA-OH macroinitiator was synthesized by ATRP utilizing a difunctional initiator containing initiating sites for both ATRP and ROP, hence creating PDMAEMA chains with one hydroxyl-functional end-group. Second, the PDMAEMA-OH was subsequently utilized as a macroinitiator for the polymerization of the less polar PCL through ROP of ε-CL from the available OH- end group. In total, three block copolymers, PDMAEMA-*block*-PCL, were produced based on the same, PDMAEMA-OH macroinitiator, and the lengths of the PCL blocks were varied by altering the ratio of PDMAEMA-OH and ε-CL. This was performed to later investigate the influence of the PCL-block length, and consequently the polarity of the block copolymers, on the surface energy of the modified surfaces and the adhesion of block copolymer-modified surfaces toward a PCL surface. In the final step, the PDMAEMA block was quaternized using MeI, leading to charged blocks with charged units that are less sensitive to changes in pH and electrolyte concentration, and a

Scheme 1. Polymerization and Quaternization of the Block Copolymers[a]

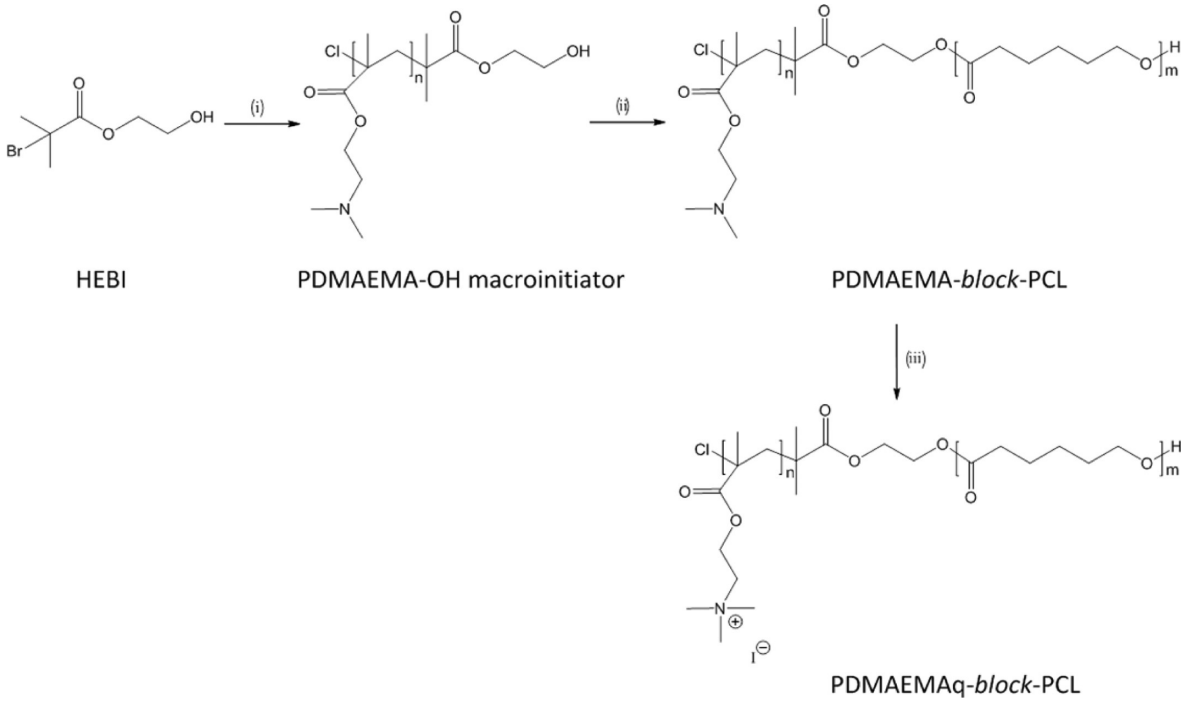

[a](i) ATRP: DMAEMA, Cu(I)Cl, HMTETA, acetone, 50 °C; (ii) ROP: ε-CL, $Sn(Oct)_2$, toluene, 85 °C; (iii) quaternization: MeI, THF, RT.

dx.doi.org/10.1021/am301981r | ACS Appl. Mater. Interfaces 2012, 4, 6796−6807

Table 3. Total M_n, M_n for PCL Blocks, $Đ_M$, T_g, T_m, and X_c for the Synthesized Polymers

sample	M_n[a] (g/mol)	$M_{n,\ PCL\ block}$[b] (g/mol)	$Đ_M$[a]	T_g[c] (°C)	T_m[c] (°C)	$X_{c,\ PCL\ block}$[d] (%)
PDMAEMA-OH	3800	-	1.24	10.1	-	-
PDMAEMA-*block*-PCL-s	11900	8100	1.14	-	51.4	72
PDMAEMA-*block*-PCL-m	17300	13 500	1.13	-	54.5	69
PDMAEMA-*block*-PCL-l	34900	31 100	1.28	-	56.0	58

[a]Measured with SEC. [b]Estimated from SEC. [c]Measured with DSC. [d]Determined from DSC according to eq 1 and normalized to the weight fraction of PCL given by SEC.

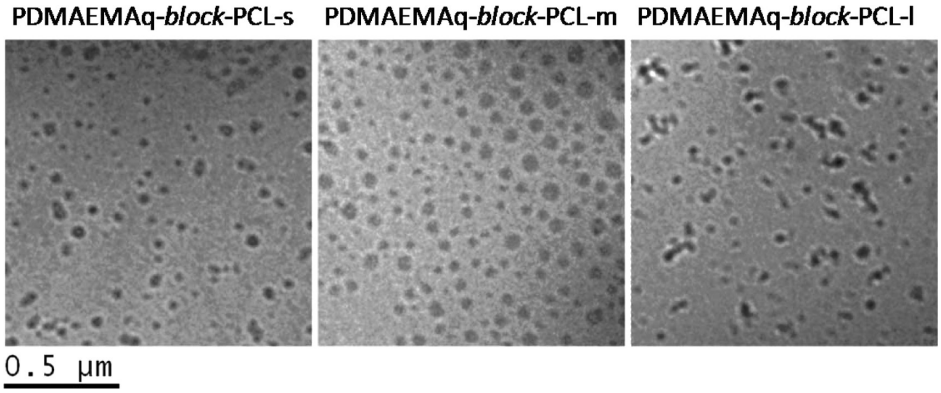

Figure 1. Cryo-TEM images of the dispersions in water of micelles from the different block copolymers.

noncharged PCL block. The purpose with the charged block was to facilitate water dispersibility and physical adsorption to oppositely charged surfaces, such as cellulose-based fibers/fibrils. The synthetic approach is shown in Scheme 1.

Polymer Characterization and Properties in Solution. To verify that the appropriate polymers were formed, i.e., PDMAEMA-OH macroinitiator and three PDMAEMA-*block*-PCL polymers, ^{1}H NMR spectroscopy was used. The spectra for all four polymers can be seen in Supporting Information, Figure S1, and these results clearly show that the macroinitiator PDMAEMA-OH and the block copolymers of PDMAEMA-block-PCL were successfully prepared. However, due to the fact that PDMAEMA is less soluble than PCL in the NMR solvent used ($CDCl_3$), the integrals of the peaks are not fully reliable and a molecular weight determination of the polymers from NMR would not be, as a consequence, reliable either. SEC was, therefore, used for all four polymers to determine both molecular weight (M_n) and dispersity ($Đ_M$). The results are shown in Table 3 and Figure S2 in the Supporting Information. As can be seen, $Đ_M$ values are all close to one, which is expected since both ATRP and ROP are controlled polymerization techniques, yielding uniform polymers. As anticipated, the molecular weights of the PDMAEMA-*block*-PCL polymers increased with increasing targeted DPs of the PCL block.

DSC was used to investigate the melting and crystallization behavior of the polymers, Table 3. The macroinitiator, PDMAEMA-OH, showed a glass transition temperature (T_g) of 10 °C, whereas for the three block copolymers, PDMAEMA-*block*-PCL, no T_g could be observed since the signal was too weak compared to the PCL signal. This is probably because the fraction of PDMAEMA in the block copolymers is low and all the block copolymers therefore show a thermal behavior similar to that of the homopolymer of PCL, which has a T_g of about −60 °C.[40] However, due to the lower temperature limit of −60 °C of the instrument this was difficult to measure, and hence no T_g was detected. With increasing length of the PCL block in the block copolymers, a slightly higher melting temperature (T_m) was observed; the higher the fraction of PCL in the sample the more similar was the behavior to that of neat PCL, which has a T_m of about 60 °C.[40] Concerning the degree of crystallinity of the PCL block in the three block copolymers, which was determined from DSC according to eq 1 and normalized to the weight fraction of PCL given by SEC, it can be said that all were found to be semicrystalline. Furthermore, the crystallinity decreases with increasing length of the PCL block and both this trend, and the range of values, are in accordance with linear well-defined neat PCL reported earlier.[41] This indicates that the semicrystalline character contributed from the PCL block is maintained in the solid state.

Since quaternized PDMAEMA is easily soluble in water but pure PCL is insoluble in water, the block copolymers were expected to form cationic micelles[42] in water under certain conditions. Cryo-TEM images were captured to study whether the block copolymers did form micelles in water, and these images are shown in Figure 1. The size of the dark gray areas in the images, which probably corresponds to the dense PCL core of the block copolymer micelles, was mostly in the range of 30−45 nm in diameter. However, small coronas around these dark gray areas are also observed, probably due to the less dense PDMAEMAq shell surrounding the PCL core. The thickness of this corona was about 10 nm which is in good agreement with theoretical estimations of fully stretched PDMAEMAq polymers from SEC data. This would add 20 nm in diameter to the micelle sizes leading to an estimation of the micelle size in the range of 50−65 nm, which is in reasonable agreement with DLS data shown in Table 4. Since DLS measures the hydrated size of the micelles, and the shell of the formed micelles were expected to be hydrated due to the charged blocks, DLS was expected to show a larger size than observed in the cryo-TEM images.

DLS was used to measure the hydrodynamic radius (R_h) of the micelles, and the values are shown in Table 4. The measurements of 100 mg/L dispersions show single peaks, and the values presented are peak values of measurements at room

Table 4. Measured Charge Density, Theoretical Ratio of Quaternized Groups in PDMAEMA Blocks, and Hydrodynamic Radius in Water of the Block Copolymer Micelles

sample	charge density, measured (meq/g)[a]	ratio, quaternized groups in PDMAEMA[b]	R_h (nm)[c]
PDMAEMAq-*block*-PCL-s	0.30	0.17	48 ± 1.1
PDMAEMAq-*block*-PCL-m	0.19	0.27	49 ± 0.6
PDMAEMAq-*block*-PCL-l	0.10	0.27	42 ± 0.6

[a]Measured with PET. [b]Calculated from added amounts of PDMAEMA-*block*-PCL and MeI in the quaternization step. [c]Measured with DLS.

temperature. The full spectra can be found in Figure S3 in the Supporting Information. The R_h values for the micelles assembled from the block copolymers appear to be relatively constant and independent of the length of the PCL block. Measurements were also performed for PDMAEMAq-*block*-PCL-m at 4 different concentrations between 100 mg/L and 1000 mg/L, which showed no significant change in size of the micelles with the concentration of the dispersions in this range. The number of block copolymers in each micelle most likely differs between the micelles being determined mainly by the attractive forces in the core of the micelles and the repulsive forces between the charged polyelectrolytes in the charged shell. The total force keeping these micelles together will probably vary depending on the balance between these forces, and this will in turn affect the behavior of the micelles at interfaces.

Charge densities of the block copolymer micelles were measured in water using PET, and the results are shown in Table 4. The block copolymers consist of a charged, relatively short, cationic block and a noncharged PCL block. Consequently, a longer noncharged PCL block results in a lower total charge density of the entire polymer since the charge is normalized with respect to the total molecular weight of the polymer. The correlation between the ratio of the lengths of the different blocks and the charge density of the block copolymers is good, i.e., a longer noncharged PCL block leads to a proportionally lower measured charge density of the entire block copolymer. The theoretical maximum charge density of

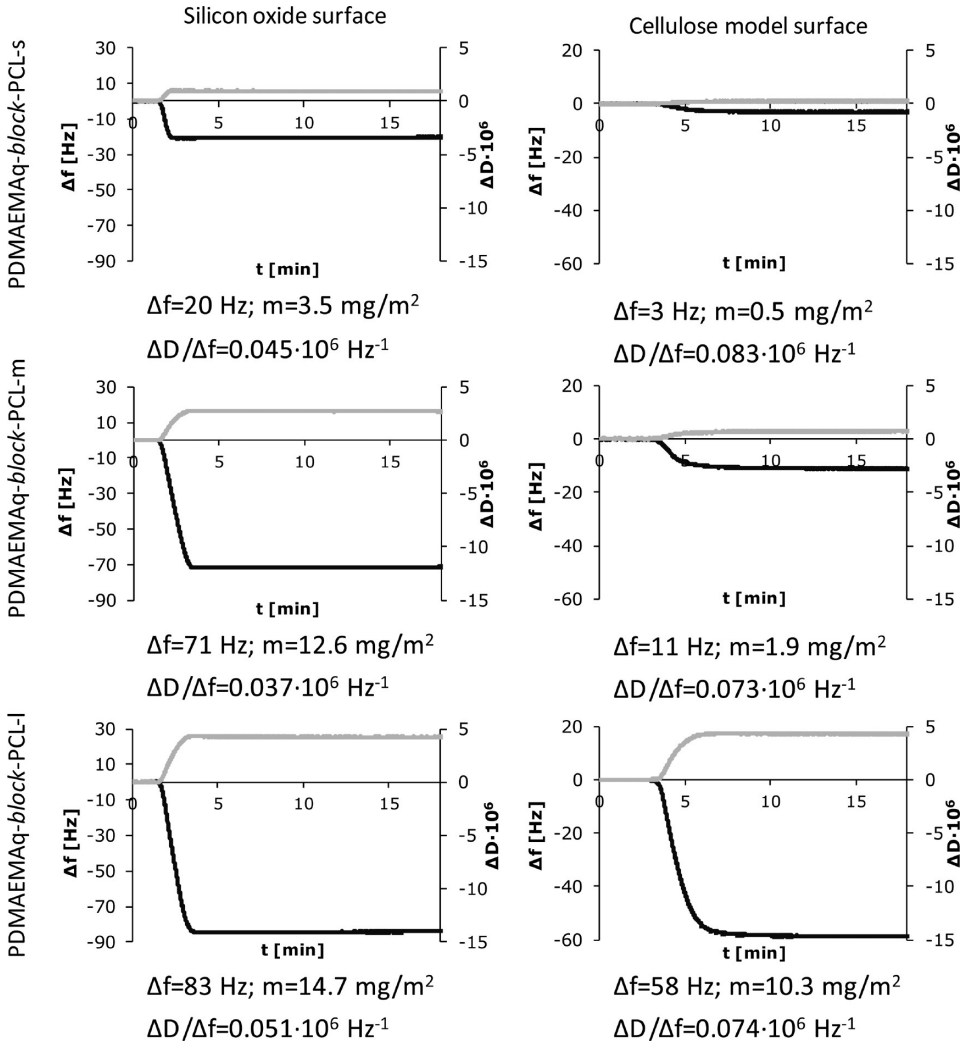

Figure 2. QCM-D data from the third overtone showing the adsorption behavior of the three block copolymers on silicon oxide surfaces (left) and on cellulose model surfaces (right). The left *y*-axis shows the normalized frequency change (black lines), and the right *y*-axis shows the change in dissipation (gray lines). ΔD/Δf values were obtained after equilibration during rinsing.

fully quaternized PDMAEMA, with iodine as counterion, is 3.3 meq/g. A higher total charge density leads to more electrostatic contact points per polymer which will most likely lead to a stronger attachment to a surface. However, a higher total charge density will also lead to lower adsorbed amount since there will be more charges per mass unit of the polymers. Therefore, the balance between strong attachment and adsorbed amounts needs to be considered when designing these kinds of polymers. The theoretical ratios between quaternized PDMAEMA groups and total amount of PDMAEMA groups for the block copolymers, displayed in Table 4, show that the block copolymers are only partly quaternized which will lead to a lower overall charge than if the block copolymers were fully quaternized, and consequently to a higher saturation adsorption which is important for these systems. It should also be noted that the measured charge density decreases as the length of the PCL block increases and from the theoretical charge density values it is clear that basically all charged groups are available for the titrating polyelectrolyte.

Properties of the Block Copolymers at Interfaces. In this work, two different substrates were investigated. Silicon oxide surfaces were used since they are anionically charged, smooth, homogeneous, hydrophilic, and well characterized[43,44] which makes them good model surfaces for cellulose-based materials. Cellulose model surfaces were also used since they are a more relevant substrate, with a stronger link to cellulose-based materials, such as cellulose-based fibers/fibrils. The adsorption of the three block copolymers was investigated with QCM, both to silicon oxide surfaces and to cellulose model surfaces. All measurements were performed using concentrations of 100 mg/L of the block copolymers in water with no added salt and a pH about 8, and the results are shown in Figures 2 and 3.

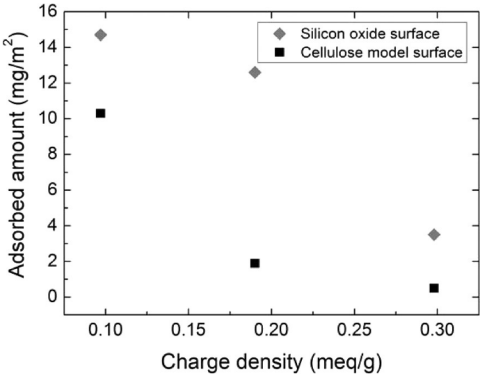

Figure 3. Adsorbed amount as a function of charge density of the block copolymer micelles on silicon oxide surfaces and on cellulose model surfaces.

As can be seen, there is a clear trend that the block copolymers with longer PCL blocks give rise to a greater adsorption on both types of surfaces. One reason for this is probably that the block copolymers with longer PCL blocks have a lower overall charge density, leading to a greater adsorption since the polymers then have more mass per unit charge and the balance of charges between the surface and the polyelectrolyte is probably the main driving force for the adsorption. However, this does not fully explain the behavior since, if there were only a pure electrostatic contribution to the adsorption, the ratio of adsorbed mass between the different block copolymer micelles should be the same for both types of surfaces and the adsorption behavior in Figure 3 should follow an 1/x trend.[45] Since this is not the case for the silicon oxide surfaces there are strong indications that also nonelectrostatic interactions, such as van der Waals forces, play an important role for the adsorption of the polymers on this substrate. The adsorption behavior on the cellulose surfaces followed this 1/x trend better, indicating a greater contribution of pure electrostatic interactions. There are still significant amounts adsorbed in all cases, especially for PDMAEMA-*block*-PCL-l, which could possibly be increased further with some added electrolyte.[18,46] Surface charge densities of the two different substrates might be different under these experimental conditions, but this should rather be reflected on the absolute adsorbed amounts and not on the shape of the curves to such an extent. To obtain information about the viscoelastic properties of the attached micelles on the various surfaces, dissipation normalized with respect to frequency, $\Delta D/\Delta f$, can be analyzed for the different systems, as shown in Figure 2. $\Delta D/\Delta f$ is quite similar for the three different micelles on the silicon oxide surfaces and also for the three different micelles on the cellulose model surfaces, but there is a significant difference between the values of the silicon oxide surfaces and of the cellulose model surfaces. The values are lower for the micelles attached to the silicon oxide surfaces, indicating that they are more rigidly attached to this type of surface than to the cellulose model surfaces. This is also evident in the data in Figure 3 which indicates that the attachment to the cellulose model surfaces is mainly driven by electrostatic interactions, while the adsorption to the silicon oxide surfaces is driven by both electrostatic interactions and nonelectrostatic contributions such as van der Waals forces.

AFM images were captured for silicon oxide surfaces before and after heat treatment at 160 °C for 2 h, and the results are shown in Figure 4. As noted previously, PCL has a T_g of about −60 °C and a T_m of about 60 °C,[40] so heat treatment was performed to enable the block copolymers to properly melt/soften and spread out on the surface in order to minimize the surface energy. The images of the three block copolymer micelles adsorbed to silicon oxide substrates show that different surface structures were obtained. The two block copolymers with shorter PCL blocks show some structure when adsorbed on the substrates before heat treatment, but no structure of micelles could be detected as found in the cryo-TEM and DLS measurements. One plausible explanation for this is that these micelles are internally weakly bound in water due to the osmotic pressure present from the charged shell. Upon contact with the surface, this structure spontaneously unfolds due to a disruption by the attractive forces on the surface, leading to a relatively smooth surface. When these surfaces are heat treated, this relatively subtle structure disappears completely, and an even smoother surface appears. However, PDMAEMAq-*block*-PCL-l showed a clear micelle structure when adsorbed onto the surface. An explanation for this could be that the PCL block was long enough in this case, leading to stronger attractive intermolecular forces within the micelles than the surface interactions. This could also be a reason why the adsorption of PDMAEMAq-*block*-PCL-l was different from PDMAEMAq-*block*-PCL-m and PDMAEMAq-*block*-PCL-s, resulting in intact micelles on the surface. The size of the PDMAEMAq-*block*-PCL-l micelles was at most about 80 nm in diameter, which is in reasonable agreement with both DLS and cryo-TEM data.

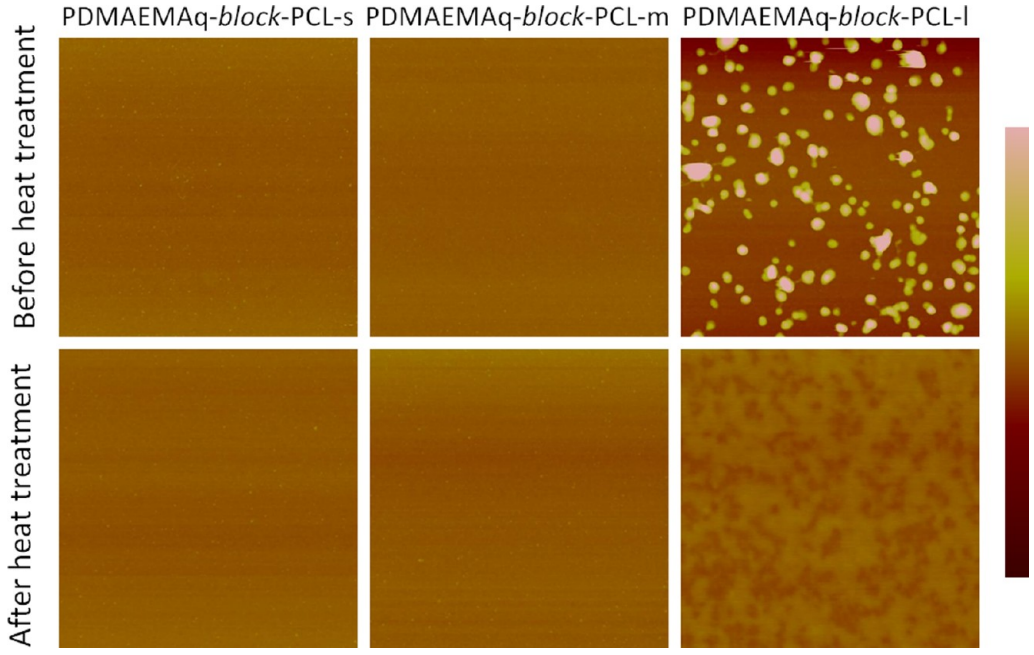

Figure 4. AFM height images of silicon oxide surfaces treated with the three block copolymer dispersions before (upper) and after (lower) heat treatment. The length of the PCL blocks increases from left to right. Images are 2 × 2 μm and the z-range is 50 nm.

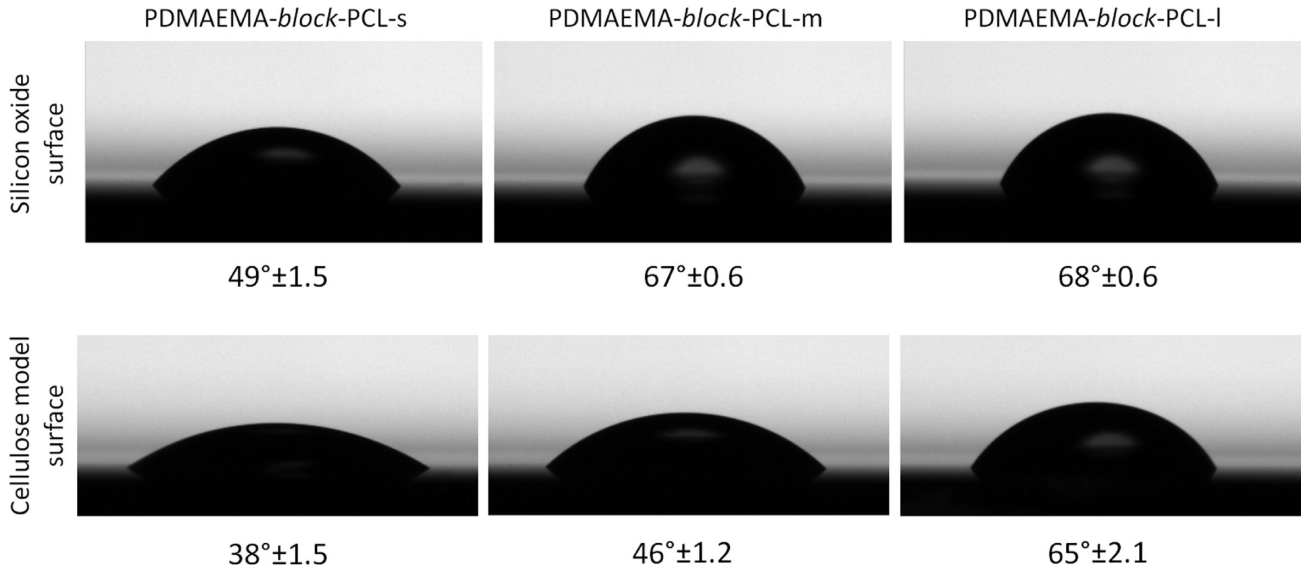

Figure 5. Contact angle of water on block copolymer modified silicon oxide surfaces (upper) and cellulose model surfaces (lower) after heat treatment. The length of the PCL blocks increases from left to right. The measurements were performed at 50% RH and 23 °C.

After heat treatment, a clear melting/softening and subsequent spreading of the micelles was observed. This was expected since the melting point of PCL is about 60 °C, which is significantly lower than the temperature used for the heat treatment.

Contact angles were measured after heat treatment for both the silicon oxide surfaces and cellulose model surfaces, and the results are shown in Figure 5. The general trend was for the surfaces treated with block copolymers with longer PCL blocks to lead to surfaces with higher contact angles against water. One factor contributing to the difference in contact angle is probably the difference in length of the PCL blocks, where a block copolymer with a longer PCL block should be able to increase the contact angle more than one with a shorter PCL block, provided that the block copolymers spread at the interface. Another parameter that probably has a large influence on the final contact angle is the amount of block copolymer that is attached to the surface, since a high attached amount should lead to a better coverage of PCL blocks on the surface, and thereby a higher contact angle. The contact angles for water on the modified cellulose model surfaces were generally smaller than those on the silicon oxide surfaces and this seems to correlate well with the smaller amounts adsorbed onto these surfaces according to the QCM measurements. The smaller contact angle with smaller adsorbed amounts was especially pronounced for the two cellulose model surfaces modified with PDMAEMAq-*block*-PCL-s and PDMAEMAq-*block*-PCL-m, while the surface treated with PDMAEMAq-*block*-PCL-l still had a relatively high adsorption leading to a relatively high

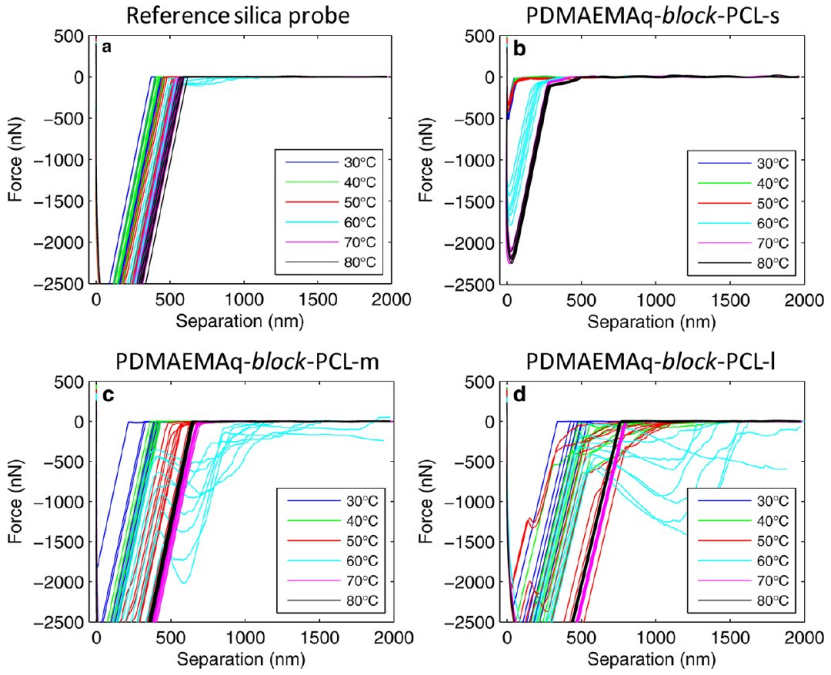

Figure 6. Force-separation curves performed at different temperatures for a reference silica probe (a), a silica probe modified with PDMAEMAq-*block*-PCL-s (b), a silica probe modified with PDMAEMAq-*block*-PCL-m (c), and a silica probe modified with PDMAEMAq-*block*-PCL-l (d).

contact angle. There seemed also to be an upper limit of contact angle that it was possible to reach, close to 70°, which is quite close to the contact angle for pure PCL which is about 70°,[47,48] indicating that a close to fully covered surface has been obtained, mainly due to a minimization of surface energy during the heat treatment.

Adhesive Behavior of the Block Copolymers. AFM colloidal probe force measurements were performed in order to investigate the adhesive properties of the three different block copolymers, i.e., to investigate whether the block copolymers can act to improve the adhesive behavior between a silica probe and a PCL surface. The measurements were performed between a PCL surface, prepared by spin coating PCL onto a silicon wafer and silica probes modified with the different block copolymers, as described in the instrumental section, i.e., block copolymers physically adsorbed onto the silica probes from aqueous dispersions with subsequent heat treatment. A nonmodified silica probe was used as a reference. The force measurements were performed at different temperatures between 30 and 80 °C with 10 degrees between the steps, with a 10 s contact time. Different temperatures in this range were used since pure PCL is a semicrystalline polymer with a melting temperature of about 60 °C. The values presented are average values of measurements performed at 6 to 9 different positions on the surface.

The force-separation curves at the different temperatures and for the different probes are shown in Figure 6. There are two main parameters that should affect the adhesion besides the molecular contact area. The first is the surface energy, where a high surface energy should lead to a higher adhesion.[11] The second is physical entanglements between the PCL blocks on the probe and the PCL on the surface, where more and stronger entanglements should lead to a stronger adhesion. During modification, the surface energy is decreased and this should lead to a lower adhesion, but the adhesive contributions from physical entanglements should increase the adhesion. The total adhesion should therefore mainly be a balance between these two parameters and the molecular contact area, which is assumed to be similar between the different block copolymers. Using the nonmodified silica probe against the PCL surface, a significant adhesion was observed at all temperatures. An increasing trend with increasing temperature was also observed, which is probably a result of a softening of the PCL surface, and hence a larger molecular contact area as the melting point is approached, and a continuing softening after the melting point which increases the interactions between the surfaces. At 60 °C, some disentanglement behavior was observed in some cases which was probably due to some of the PCL becoming physically attached to the silica probe and being detached during separation. However, these were very weak forces and occurred only in some of the measurements, but they still show that there are significant adhesive forces between PCL and silica, probably because silica has a relatively high surface energy.

For the silica probe modified with PDMAEMAq-*block*-PCL-s, relatively low pull-off forces were observed up to 50 °C, which could be partly due to a decreased surface energy. The pull-off force was significantly higher at 60 °C, and some entanglement behavior was observed as a small tail in the force-separation curves for all the measurements. Both the pull-off force and the entanglement behavior continued to increase slightly at 70 and 80 °C, and at these temperatures the maximum separation distance was approximately 500 nm. The block copolymer in its most extended form is significantly shorter than this distance, indicating that not only do PCL blocks from the modified probe reach into the PCL surface but also that some kind of deformation of the PCL surface occurs during the separation. This means that PCL molecules probably protrude from the surface during the separation.

With the silica probe modified with PDMAEMAq-*block*-PCL-m, relatively high pull-off forces were measured, similar to those with the nonmodified silica probe, up to 60 °C.

dx.doi.org/10.1021/am301981r | ACS Appl. Mater. Interfaces 2012, 4, 6796−6807

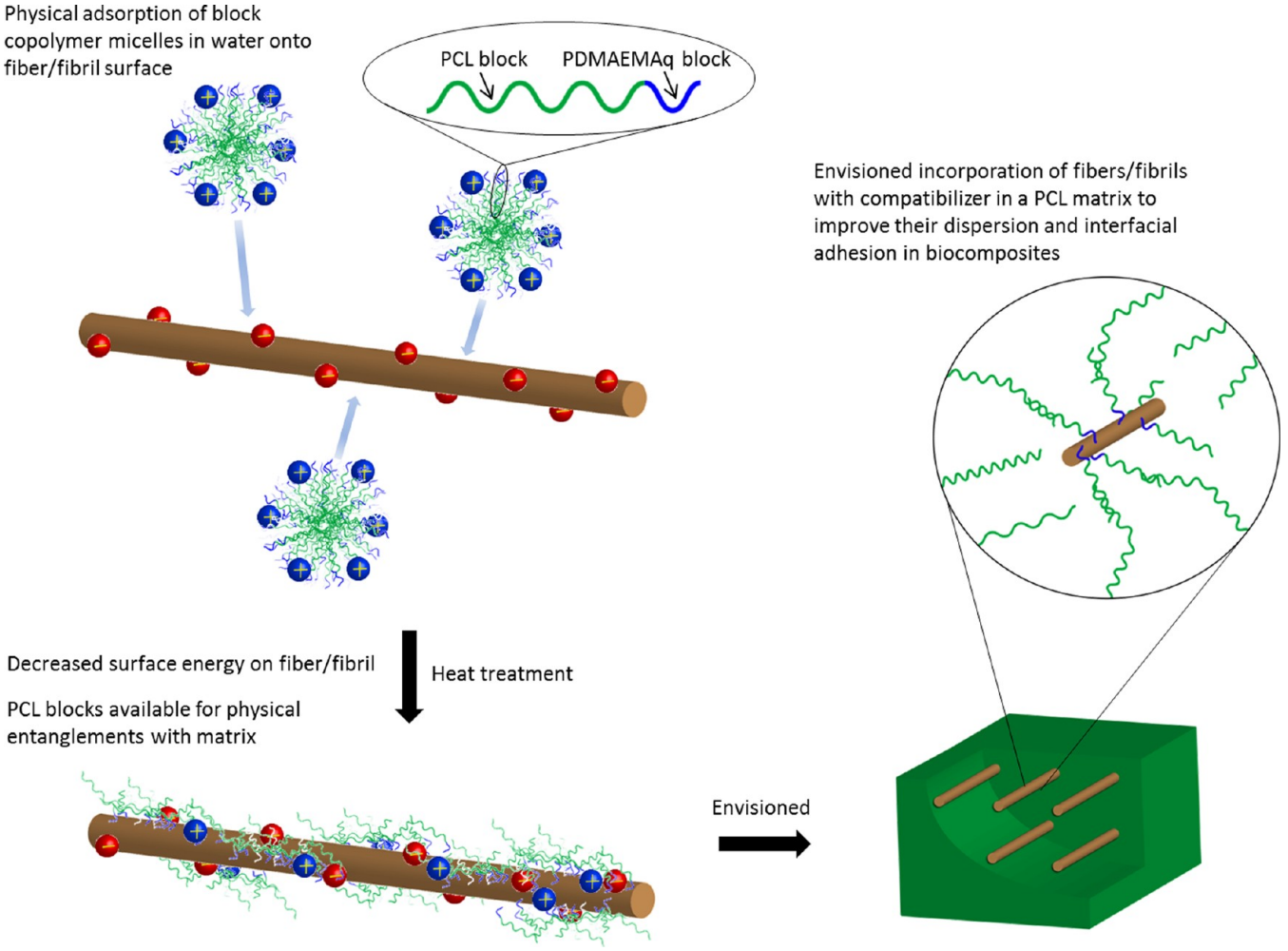

Figure 7. Illustration of how the block copolymer micelles are adsorbed onto a fiber/fibril surface and is envisioned to improve interactions between cellulose fibers/fibrils and PCL in a biocomposite.

Thereafter, at 70 and 80 °C, the pull-off force increased significantly, more than with the nonmodified silica probe, indicating a stronger joint being formed, mainly due to physical entanglements between the surfaces. The force-separation curves indicate that small entanglements were present already at 50 °C. The entanglement behavior was enhanced significantly at 60 °C, where a clear disentanglement process was observed during separation out to approximately 2 μm. However, at 70 and 80 °C, no disentanglements were observed. This may be due both to a higher pull-off force, leading to a stronger initial dissociation event of the surfaces, and to a higher mobility of the polymers at the higher temperatures, leading to a faster and easier disentanglement. All the entanglements formed in the joint during contact may therefore be disentangled very rapidly during this dissociation event, and they are therefore not visible in the force-separation curves. Similar behavior has also been reported for PMMA surfaces.[49]

With the silica probe modified with PDMAEMAq-*block*-PCL-l, relatively high pull-off forces were measured, similar to those with the nonmodified silica probe, up to 60 °C. Thereafter, at 70 and 80 °C, the pull-off force increased significantly more than for the nonmodified silica probe, indicating a stronger joint, mainly due to physical entanglements between the surfaces, as in the case with PDMAEMAq-*block*-PCL-m. Some signs of entanglements were observed already at 40 °C. The entanglement behavior was enhanced at 50 °C and significantly more enhanced at 60 °C, where a clear disentanglement process was observed during separation out to approximately 2 μm. At 60 °C, the forces during this disentangling process were significantly higher than with the PDMAEMAq-*block*-PCL-m and much higher than with the PDMAEMAq-*block*-PCL-s. The strength of the entanglements clearly increased with increasing molecular weight of the PCL block. A similar entanglement behavior has been shown earlier for PCL grafted onto cellulose spheres.[50] At 70 and 80 °C no disentanglements were observed, probably for the same reason as proposed for PDMAEMAq-*block*-PCL-m. It is also very interesting to note that the physical adsorption, formed by this type of block copolymer, was strong enough to improve the adhesion between the surfaces under these conditions.

These measurements were performed mainly to see whether this type of block copolymer can introduce entanglements into a PCL matrix. The absolute values give some information about the adhesive behavior, but they are less significant in a real system since the system would be cooled after the entanglements had been formed at a higher temperature, and this would significantly increase the adhesion. If the material is used at room temperature, which is below the melting temperature, the entangled PCL blocks would probably

dx.doi.org/10.1021/am301981r | ACS Appl. Mater. Interfaces 2012, 4, 6796−6807

cocrystallize with the PCL matrix, and this would significantly increase the adhesion.

An illustration of how the block copolymer micelles are adsorbed onto a cellulose-based fiber/fibril surface and is thought to act as a compatibilizer between the fiber/fibril and a PCL matrix in a biocomposite, both by decreasing the surface energy of the fiber/fibril surface and by introducing polymer entanglements to the PCL matrix, is given in Figure 7.

CONCLUSIONS

Three different amphiphilic block copolymers for use as compatibilizers in biocomposites were synthesized and evaluated. The cationic PDMAEMA block was synthesized using ATRP and was subsequently quaternized using MeI, and the PCL blocks with different lengths were synthesized using ROP to give PDMAEMAq-*block*-PCL. These block copolymers self-assemble in water into cationic micelles which are adsorbed onto anionic surfaces such as cellulose fibers/fibrils. After a heat treatment, the contact angle of these surfaces increased significantly, and the block copolymers with longer PCL blocks showed contact angles for water close to those of pure PCL surfaces. AFM force measurements showed a clear entanglement behavior between these block copolymers and a PCL surface, which is important for the formation of an adhesive interface between the reinforcing material and the matrix in the final biocomposite. The results of this work show that it is possible to electrostatically adsorb a cationic compatibilizer onto an anionic reinforcing material in water under mild conditions and that it can both decrease the surface energy of the surface to which it adsorbs to and introduce molecular entanglements to a polymer matrix to give improved adhesion at the interface. This type of compatibilizer could be interesting for a wide range of applications, where one of the most interesting applications is as a compatibilizer between cellulose-based fibers/fibrils and a less polar matrix such as PCL, to improve the mechanical properties of these biocomposites.

ASSOCIATED CONTENT

Supporting Information

^{1}H NMR data, full SEC data, and more detailed DLS data. This material is available free of charge via the Internet at http://pubs.acs.org.

AUTHOR INFORMATION

Corresponding Author

*Phone: +46 8 7908296. E-mail: utsel@kth.se.

Author Contributions

[§]Both authors contributed equally to the experimental work.

Notes

The authors declare no competing financial interest.

ACKNOWLEDGMENTS

BiMaC Innovation is gratefully acknowledged for financial support. The Wallenberg Wood Science Centre (WWSC) is also acknowledged for financial support. Gunnel Karlsson at Biomicroscopy Unit, Lund University, is acknowledged for the cryo-TEM work.

REFERENCES

(1) Klemm, D.; Kramer, F.; Moritz, S.; Lindström, T.; Ankerfors, M.; Gray, D.; Dorris, A. *Angew. Chem., Int. Ed.* **2011**, *50*, 5438−5466.
(2) Bledzki, A. K.; Gassan, J. *Prog. Polym. Sci.* **1999**, *24*, 221−274.
(3) George, J.; Sreekala, M. S.; Thomas, S. *Polym. Eng. Sci.* **2001**, *41*, 1471−1485.
(4) Gardner, D. J.; Oporto, G. S.; Mills, R.; Samir, M. *J. Adhes. Sci. Technol.* **2008**, *22*, 545−567.
(5) Felix, J. M.; Gatenholm, P. *J. Appl. Polym. Sci.* **1993**, *50*, 699−708.
(6) Tingaut, P.; Zimmermann, T.; Lopez-Suevos, F. *Biomacromolecules* **2010**, *11*, 454−464.
(7) Kato, K.; Uchida, E.; Kang, E. T.; Uyama, Y.; Ikada, Y. *Prog. Polym. Sci.* **2003**, *28*, 209−259.
(8) Bhattacharya, A.; Misra, B. N. *Prog. Polym. Sci.* **2004**, *29*, 767−814.
(9) Gamstedt, E. K.; Sandell, R.; Berthold, F.; Pettersson, T.; Nordgren, N. *Mech. Mater.* **2011**, *43*, 693−704.
(10) Lönnberg, H.; Larsson, K.; Lindström, T.; Hult, A.; Malmström, E. *ACS Appl. Mater. Interfaces* **2011**, *3*, 1426−1433.
(11) Creton, C.; Kramer, E. J.; Hui, C. Y.; Brown, H. R. *Macromolecules* **1992**, *25*, 3075−3088.
(12) Matyjaszewski, K.; Xia, J. H. *Chem. Rev.* **2001**, *101*, 2921−2990.
(13) Wang, J. S.; Matyjaszewski, K. *Macromolecules* **1995**, *28*, 7901−7910.
(14) Braunecker, W. A.; Matyjaszewski, K. *Prog. Polym. Sci.* **2007**, *32*, 93−146.
(15) Matyjaszewski, K.; Tsarevsky, N. V. *Nat. Chem.* **2009**, *1*, 276−288.
(16) Hems, W. P.; Yong, T.-M.; van Nunen, J. L. M.; Cooper, A. I.; Holmes, A. B.; Griffin, D. A. *J. Mater. Chem.* **1999**, *9*, 1403−1407.
(17) Gaucher, G.; Dufresne, M.-H.; Sant, V. P.; Kang, N.; Maysinger, D.; Leroux, J.-C. *J. Controlled Release* **2005**, *109*, 169−188.
(18) Utsel, S.; Carlmark, A.; Pettersson, T.; Bergström, M.; Malmström, E. E.; Wågberg, L. *Eur. Polym. J.* **2012**, *48*, 1195−1204.
(19) Pettersson, T.; Utsel, S.; Wagberg, L. *Rev. Sci. Instrum.* **2012**, *83*, 106107−106103.
(20) Lönnberg, H.; Fogelström, L.; Zhou, Q.; Hult, A.; Berglund, L.; Malmström, E. *Compos. Sci. Technol.* **2011**, *71*, 9−12.
(21) Kricheldorf, H. R.; Berl, M.; Scharnagl, N. *Macromolecules* **1988**, *21*, 286−293.
(22) Jakubowski, W.; Lutz, J.-F.; Slomkowski, S.; Matyjaszewski, K. *J. Polym. Sci., Part A: Polym. Chem.* **2005**, *43*, 1498−1510.
(23) Motala-Timol, S.; Jhurry, D. *Eur. Polym. J.* **2007**, *43*, 3042−3049.
(24) Carlmark, A.; Malmstrom, E. E. *Biomacromolecules* **2003**, *4*, 1740−1745.
(25) Woodruff, M. A.; Hutmacher, D. W. *Prog. Polym. Sci.* **2010**, *35*, 1217−1256.
(26) Herrick, F. W.; Casebier, R. L.; Hamilton, J. K.; Sandberg, K. R. *J. Appl. Polym. Sci.: Appl. Polym. Symp.* **1983**, *37*, 797−813.
(27) Turbak, A. F.; Snyder, F. W.; Sandberg, K. R. *J. Appl. Polym. Sci.: Appl. Polym. Symp.* **1983**, *37*, 815−827.
(28) Wågberg, L.; Decher, G.; Norgren, M.; Lindström, T.; Ankerfors, M.; Axnäs, K. *Langmuir* **2008**, *24*, 784−795.
(29) Wunderlich, B. *Macromolecular Physics, Vol. 3: Crystal Melting*; Academic Press, Inc.: New York, 1980.
(30) Horn, D. *Prog. Colloid Polym. Sci.* **1978**, *65*, 251−264.
(31) Aulin, C.; Ahola, S.; Josefsson, P.; Nishino, T.; Hirose, Y.; Österberg, M.; Wågberg, L. *Langmuir* **2009**, *25*, 7675−7685.
(32) Marx, K. A. *Biomacromolecules* **2003**, *4*, 1099−1120.
(33) Sauerbrey, G. *Z. Phys.* **1959**, *155*, 206−222.
(34) Aulin, C.; Varga, I.; Claesson, P. M.; Wågberg, L.; Lindström, T. *Langmuir* **2008**, *24*, 2509−2518.
(35) Ducker, W. A.; Senden, T. J.; Pashley, R. M. *Nature* **1991**, *353*, 239−241.
(36) Ducker, W. A.; Senden, T. J.; Pashley, R. M. *Langmuir* **1992**, *8*, 1831−1836.
(37) Sader, J. E.; Chon, J. W. M.; Mulvaney, P. *Rev. Sci. Instrum.* **1999**, *70*, 3967−3969.
(38) Pettersson, T.; Nordgren, N.; Rutland, M. W. *Rev. Sci. Instrum.* **2007**, *78*, 093702−093708.

(39) Huang, J. Y.; Koepsel, R. R.; Murata, H.; Wu, W.; Lee, S. B.; Kowalewski, T.; Russell, A. J.; Matyjaszewski, K. *Langmuir* **2008**, *24*, 6785−6795.
(40) Averous, L. *J. Macromol. Sci., Polym. Rev* **2004**, *C44*, 231−274.
(41) Nunez, E.; Ferrando, C.; Malmström, E.; Claesson, H.; Werner, P. E.; Gedde, U. W. *Polymer* **2004**, *45*, 5251−5263.
(42) Talingting, M. R.; Ma, Y. H.; Simmons, C.; Webber, S. E. *Langmuir* **2000**, *16*, 862−865.
(43) Bolt, G. H. *J. Phys. Chem.* **1957**, *61*, 1166−1169.
(44) Vigil, G.; Xu, Z. H.; Steinberg, S.; Israelachvili, J. *J. Colloid Interface Sci.* **1994**, *165*, 367−385.
(45) Vandesteeg, H. G. M.; Stuart, M. A. C.; Dekeizer, A.; Bijsterbosch, B. H. *Langmuir* **1992**, *8*, 2538−2546.
(46) Fleer, G. J. *Polymers at interfaces*, 1st ed.; Chapman & Hall: London, 1993; Chapter 7.
(47) Biresaw, G.; Carriere, C. J. *J. Polym. Sci., Part B: Polym. Phys.* **2001**, *39*, 920−930.
(48) Liu, L.; Guo, S. R.; Chang, J.; Ning, C. Q.; Dong, C. M.; Yan, D. Y. *J. Biomed. Mater. Res., Part B* **2008**, *87B*, 244−250.
(49) Luengo, G.; Pan, J. M.; Heuberger, M.; Israelachvili, J. N. *Langmuir* **1998**, *14*, 3873−3881.
(50) Nordgren, N.; Lönnberg, H.; Hult, A.; Malmström, E.; Rutland, M. W. *ACS Appl. Mater. Interfaces* **2009**, *1*, 2098−2103.